Published in final edited form as:
J Am Chem Soc. 2013 April 17; 135(15): 5656–5668. doi:10.1021/ja311729d.

Aromatic Sulfonyl Fluorides Covalently Kinetically Stabilize Transthyretin to Prevent Amyloidogenesis while Affording a Fluorescent Conjugate

Neil P. Grimster[†,‡], **Stephen Connelly**[§,‡], **Aleksandra Baranczak**[†], **Jiajia Dong**[†], **Larissa B. Krasnova**[†], **K. Barry Sharpless**[†,‖], **Evan T. Powers**[†], **Ian A. Wilson**[§,‖], and **Jeffery W. Kelly**[†,⊥,‖]

[†]Department of Chemistry, The Scripps Research Institute, 10550 North Torrey Pines Road, La Jolla, California 92037, United States

[§]Department of Molecular Biology, The Scripps Research Institute, 10550 North Torrey Pines Road, La Jolla, California 92037, United States

[⊥]Department of Molecular and Experimental Medicine, The Scripps Research Institute, 10550 North Torrey Pines Road, La Jolla, California 92037, United States

[‖]The Skaggs Institute for Chemical Biology, The Scripps Research Institute, 10550 North Torrey Pines Road, La Jolla, California 92037, United States

Abstract

Molecules that bind selectively to a given protein and then undergo a rapid chemoselective reaction to form a covalent conjugate have utility in drug development. Herein a library of 1,3,4-oxadiazoles substituted at the 2 position with an aryl sulfonyl fluoride and at the 5 position with a substituted aryl known to have high affinity for the inner thyroxine binding subsite of transthyretin (TTR) were conceived of by structure-based design principles and were chemically synthesized. When bound in the thyroxine binding site, most of the aryl sulfonyl fluorides react rapidly and chemoselectively with the pK_a-perturbed K15 residue, kinetically stabilizing TTR and thus preventing amyloid fibril formation, known to cause polyneuropathy. Conjugation t_{50}s range from 1 to 4 min, ~ 1400 times faster than the hydrolysis reaction outside the thyroxine binding site. X-ray crystallography confirms the anticipated binding orientation and sheds light on the sulfonyl fluoride activation leading to the sulfonamide linkage to TTR. A few of the aryl sulfonyl fluorides efficiently form conjugates with TTR in plasma. A few of the TTR covalent kinetic stabilizers synthesized exhibit fluorescence upon conjugation and therefore could have imaging applications as a consequence of the environment sensitive fluorescence of the chromophore.

1. INTRODUCTION

Transthyretin (TTR) is one of more than 30 human proteins that are known to misfold and/or misassemble into a variety of extracellular and/or intracellular aggregate morphologies linked to pathology, including the characteristic cross-β-sheet structures known as amyloid, after which the amyloid diseases or amyloidoses are named[1-8]. Compelling genetic and

Corresponding Authorjkelly@scripps.edu.
[‡]**Author Contributions** These authors contributed equally.

Protein Data Bank Accession Codes. Atomic coordinates and structure factors have been deposited in the Protein Data Bank (www.pdb.org) and are available under accession codes 4FI6 (WT-TTR in complex with **9**), 4FI7 (WT-TTR in complex with **5**) and 4FI8 (WT-TTR in complex with **15**).

pharmacologic evidence supports the hypothesis that the process of TTR amyloid fibril formation or amyloidogenesis elicits the proteotoxicity and post-mitotic tissue degradation characteristic of TTR amyloido-ses[9-16].

Transthyretin is composed of 127-amino-acid, β-sheet-rich subunits that associate into a tetrameric quaternary structure[17]. This affords two unique dimer-dimer interfaces, the more labile of which creates two thyroxine (T_4) binding sites along the z-axis (Figure 1a, b)[18]. Synthesized and secreted by the liver and choroid plexus, the established physiological functions of TTR are to transport holo retinol-binding protein and thyroid hormone T_4 in the blood and cerebrospinal fluid (CSF)[19,20]. Due to the presence of thyroid binding globulin and albumin, the vast majority (>99%) of the TTR T_4 binding sites are unoccupied in human blood.

Rate-limiting tetramer dissociation yields folded monomers that must then undergo partial denaturation to aggregate, yielding a variety of aggregate structures, including amyloid fibrils[13,14,18,21-30]. In contrast to the nucleated polymerization or nucleated conformational conversion mechanisms that govern the aggregation of many amyloidogenic proteins[31], TTR amyloidogenesis occurs via a thermodynamically favorable or downhill aggregation reaction[32]. The aggregation of wild-type transthyretin (WT-TTR) is the underlying cause of senile systemic amyloidosis (SSA), a cardiomyopathy thought to affect 15% of the male population over the age of 65[16,33-35]. Aggregation of the V122I-TTR mutant, found in 3-4 % of Africans, causes familial amyloid cardiomyopathy (FAC)[15]. Familial amyloid polyneuropathy (FAP), a peripheral neuropathy, results from the aggregation of one of over one hundred TTR mutations, of which the V30M mutation is the most common[5,9,10,36].

To date, we have synthesized over 1000 non-covalent, small molecule TTR kinetic stabilizers, molecules that bind to the T_4 binding sites, preferentially stabilizing the native tetrameric structure of TTR over its dissociative transition state, and their collective structure-activity relationships allowed us to conceive of the 1,3,4-oxadiazoles reported here (Figure 2)[37-55]. Non-covalent kinetic stabilizer binding to the tetramer renders the energy barrier for dissociation too high to surmount under physiological conditions, locking TTR in its native tetrameric structure, thus preventing aggregation[14,21,27]. Recently, one of these TTR kinetic stabilizers, the benzoxazole tafamidis, was shown to significantly slow neurodegeneration in a phase II/III placebo-controlled clinical trial in V30M-TTR FAP[12,39]. That kinetic stabilization of the TTR tetramer can ameliorate TTR amyloid disease is further supported by human genetic evidence. Incorporation of T119M-TTR trans-suppressor subunits into TTR heterotetramers, otherwise composed of FAP-TTR associated subunits, kinetically stabilizes the TTR tetramer and ameliorates FAP amyloidogenesis in Portuguese compound heterozygotes, also by making the TTR tetramer dissociation barrier insurmountable[11,14,56].

Molecules that bind selectively to a protein target and then chemoselectively modify that target have recently received renewed attention as bona fide drug candidates[57,58]. Numerous covalent drugs have received regulatory agency approval and have proven to be safe and effective[59,60]. Historically, irreversible covalent modifiers have “engendered anxiety”[58] related to off-target reactivity, which has resulted in this approach being disfavored by most medicinal chemists. Despite these concerns, the ability to permanently and selectively modify a protein of interest in a chemoselective fashion provides distinct advantages over a non-covalent strategy[44,58,61,62]. One of these is that if high binding selectivity and modification chemoselectivity can be achieved, less drug can be given per dose relative to non-covalent drug candidates[61,62]. This could be relevant for TTR kinetic stabilizers, since TTR has a > 24 h half-life, hence two small doses of a covalent kinetic stabilizer/day could be used to maximize efficacy and to minimize the possibility of off-target toxicity[44].

We recently reported a stilbene scaffold-based family of covalent small molecule TTR kinetic stabilizers that bind to the T_4 binding site of TTR and then covalently modify TTR[44]. These compounds were found to be selective for modifying TTR over the 4000+ other proteins present in blood plasma[44,63]. These covalent TTR modifiers rely on an activated ester, which is amidated by attack of the pK_a perturbed K15 ε-amino group, situated at the top of the T_4 binding site in the TTR tetramer (Figure 1c). We were interested in increasing the reaction chemoselectivity of the covalent TTR kinetic stabilizers and in producing a covalent stabilizer with benign leaving groups, unlike the phenols and thiophenols liberated from kinetic stabilizers like **1** (Figure 3) used previously[44,45].

Herein, we describe our efforts to develop small molecule covalent TTR kinetic stabilizers, utilizing an aromatic sulfonyl fluoride functional group to facilitate the covalent linkage[64-66]. Compounds represented by generic structure **2** (Figure 3) were synthesized, each having two differentially substituted aromatic rings (A and B) linked by a 1,3,4-oxadiazole. Compounds **3-18** were employed to explore the relationship between structure and the ability to covalently modify and kinetically stabilize WT-TR and the destabilized V30M-TTR homotetramers. The TTR modification selectivity of six of these compounds was subsequently investigated in human plasma[63], revealing that one compound was capable of chemoselectively modifying one of the two transthyretin T_4 binding sites *ex vivo*, a stoichiometry that kinetically stabilizes the tetrameric form of TTR[30]. To contribute to understanding the structure-activity relationship surrounding this series, three compounds of interest were co-crystallized with WT-TTR, and the high-resolution structures solved, confirming the sulfonamide linkage and revealing the common binding orientation of the biaryl 1,3,4-oxadiazoles. In addition, several of these compounds were discovered to become fluorescent upon covalently modifying TTR and their fluorescence properties were subsequently characterized.

2. EXPERIMENTAL METHODS

Evaluating the Binding Stoichiometry of Candidate Kinetic Stabilizers to Recombinant TTR

WT-TTR was expressed and purified from an *E. coli* expression system as described previously[67]. To a sample of WT-TTR (995 μL, final concentration 3.6 μM) was added a test compound (5 μL of a 1.44 mM solution in DMSO) and incubated at 25 °C. After 18 h, the sample was analyzed by reverse phase HPLC, as described previously[44], on a Waters 600 E multi-solvent delivery system, using a Waters 486 tunable absorbance detector, a 717 auto-sampler, and a Thermo Hypersil Keystone Betabasic-18 column (54mm column length, 150 Å pore size, 3 μm particle size). The "A" mobile phase comprises 0.1% TFA in 94.9% H_2O + 5% CH_3CN, and the "B" mobile phase is made up of 0.1% TFA in 94.9% CH_3CN + 5% H_2O. Linear gradients were run at 90:10 for 3 min, then 90:10 A:B to 0:100 A:B over 50 min, held at 0:100 A:B for 5 min, then re-equilibrated at 90:10 A:B for 10 min. The experiment was repeated replacing WT-TTR with V30M-TTR.

Kinetics of TTR Conjugation Reaction by HPLC Analysis

5, **9**, **15**, and **19** (5 μL, 1.44 mM solution in DMSO, final concentration 7.2 μM) were added to WT-TTR (1 mL, 0.2 mg/mL, 3.6 μM solution in 10 mM phosphate, 100 mM KCl, and 1 mM EDTA, pH 7.0) at 37 °C. An aliquot (200 μL) was removed at 2, 10, 30, 60, and 120 min and trifluoroacetic acid (TFA, 5 μL) was added to quench the reaction. The samples were subsequently analyzed by HPLC using the conditions described above.

TTR Fibril Formation Assay

To assess fibril formation, a test compound (5 μL of a 1.44 mM solution in DMSO) was added to a solution of either WT- or V30M-TTR (495 μL, 7.2 μM in 10 mM phosphate, 100

mM KCl, and 1 mM EDTA, pH 7.0) in a disposable plastic cuvette. The mixture was vortexed and incubated at room temperature. After 1 h, 500 μL of 100 mM acetate, 100 mM KCl, 1 mM EDTA, pH 4.2 was added, decreasing the pH of the assay solution to 4.4. The cuvette was sealed and incubated at 37 °C without agitation. After 3 days, the solution was vortexed to evenly distribute any precipitate and the turbidity of the solution at 400 nm was recorded using a Hewlett-Packard model 8453 UV-vis spectrophotometer.

Fluorimetric Assay with Recombinant Wild-Type Transthyretin

The covalent TTR modifiers (5 μL, 1.44 mM solution in DMSO, final concentration 7.2 μM) were added to WT-TTR homotetramer (1 mL, 0.2 mg/mL, 3.6 μM solution in 10 mM phosphate, 100 mM KCl, and 1 mM EDTA, pH 7.0) in a microfuge tube. The samples were vortexed and incubated at 25 °C. After 1 h, the fluorescence changes were monitored using a Varian Cary 50 spectrofluorometer at 37 °C in a 1-cm path length quartz cell. The excitation slit was set at 5 nm, and the emission slit was set at 5 mm. Emission spectra were collected from 390 to 700 nM, using the excitation wavelengths shown in the Table S1.

Kinetics of TTR Conjugation Reaction by Fluorescence Spectroscopy

5 (5 μL, 1.44 mM solution in DMSO, final concentration 7.2 μM) was added to WT-TTR (1 mL, 0.2 mg/mL, 3.6 μM solution in 10 mM phosphate, 100 mM KCl, and 1 mM EDTA, pH 7.0). The fluorescence emission at 520 nM was recorded (excitation 365 nM) every 6 seconds using a Varian Cary 50 spectrofluorometer at 37 °C in a 1-cm path length quartz cell. The excitation slit was set at 5 nm, and the emission slit was set at 5 mm. The experiment was also performed using **19** (excitation: 328 nM, emission: 430nM).

Quantum Yield Measurement

Compound **5** or **6** (15 μL of a 1.44 mM solution in DMSO, final concentration 7.2 μM) was added to 3 mL of a solution of WT-TTR homotetramer (0.2 mg/mL, 3.6 μM) in 10 mM phosphate, 100 mM KCl, and 1 mM EDTA, pH 7.0. The samples were vortexed and incubated for 1 h at 25 °C. Quantum yields were measured by following the instructions at www.jobinyvon.com/usadivisions/Fluorecence/applications/quantumyieldstrad.pdf. Quinine bisulfate in 0.5 M H_2SO_4 was used as a reference for comparison ($\Phi_f = 0.546$).

Evaluating the Binding Stoichiometry of Candidate Kinetic Stabilizers to TTR in Human Blood Plasma

The plasma TTR binding selectivity assay that evaluates the covalent binding stoichiometry of a test compound to TTR in human blood plasma has been previously described[44,63]. Briefly, to a sample of human blood plasma (1 mL), was added a test compound (8.9 μL of either a 0.72, 1.44, and 2.88 mM solution in DMSO) and then the plasma solution was incubated at 37 °C for 1 h. A 1:1 (v/v) slurry of un-functionalized Sepharose™ resin (134 μL) in TSA buffer (10 mM Tris, 140 mM NaCl, pH 8.0) was added, and the solution was incubated for 1 h at 4 °C on a rocker plate (18 rpm). The solution was then centrifuged, and the supernatant was divided into two aliquots (400 μL), anti-TTR antibody conjugated Sepharose™ resin (200 μL) in TSA buffer was added to each. The solution was gently rocked (18 rpm) at 4 °C for 4 h, then centrifuged (1,000×g) for 5 min, and the supernatant removed. The resin was washed three times by shaking for 10 min with TSA buffer containing 0.05% saponin (1 mL) and then thrice more with TSA buffer (1 mL). After centrifugation and removal of the supernatant, triethylamine (155 μL, 100 mM, pH 11.5) was added to the Sepharose™ resin, to dissociate the TTR and TTR-test compound complex from the resin, and the suspension was rocked (18 rpm) at 4 °C. After 30 min, the sample was centrifuged (16,000×g) for 5 min, and 145 L of the supernatant was removed, and 135 μL analyzed by reverse phase HPLC, using previously described mobile phases and linear

gradient: 90:10 for 3 min, then 90:10 A:B to 20:80 A:B over 50 min, then 0:100 A:B for 5 min, then re-equilibrated at 90:10 A:B for 10 min. The ratio of TTR to covalently modified TTR was determined from the reverse phase HPLC peak areas using standard curves.

Urea-Induced Dissociation Kinetics Study

Slow TTR tetramer dissociation is not detectable by far-UV circular dichroism (CD) spectroscopy; however, dissociation is linked to rapid (~500,000 × faster) monomer unfolding under denaturing conditions, which is easily detectable by far-UV CD spectroscopy. Test compounds (7.2 μL, at 1 mM in acetonitrile) were added to WT-TTR (200 μL, 1 mg/mL, 18 μM in 10 mM sodium phosphate buffer, 100 mM KCl, 1 mM EDTA, pH 7.0) in a microfuge tube. These mixtures were briefly vortexed and incubated at 25 °C. After 1 h, TTR-test compounds (100 μL) were added to a 6.67 M urea solution (900 μL, 10 mM sodium phosphate buffer, 100 mM KCl, and 1 mM EDTA, pH 7.0) to give a final concentration of 1.8 μM for TTR, 6 M for urea, and final concentrations of test compound of 3.6 μM (2×). The mixtures were vortexed and incubated in the dark at 25 °C without agitation. CD spectra at a final urea concentration of 6 M were measured at 215-218 nm (0.5 nm steps, 10 second averaging time, and five times scan) after 0, 5, 10, 24, 48, 72, 96, 120, and 144 h of incubation.

Crystallization and Structure Determination of the WT-TTR/Ligand Complexes

The WT-TTR protein was concentrated to 6 mg/mL in 10 mM sodium phosphate buffer and 100 mM KCl (pH 7.6) and co-crystallized at room temperature with a 2.5 molar excess of each ligand using the vapor-diffusion sitting drop method. All crystals were grown from 1.395 M sodium citrate, 3.5% v/v glycerol at pH 5.5. The crystals were cryo-protected with 10% v/v glycerol. Data were collected at beam-lines 11-1 or 12-2 at the Stanford Synchrotron Radiation Light Source (SSRL) at a wavelength of 0.9795 Å. All diffraction data were indexed, integrated, and scaled using HKL2000 in space group $P2_12_12$ with two subunits observed per asymmetric unit. The structure was determined bymolecular replacement using the model coordinates of 2FBR in the program Phaser. The modified lysine-ligand coordinates and restraints files were generated using JLigand. The covalently modified lysine residues were assigned an occupancy of 0.5 to account for the positions on the incident 2-fold symmetry axis z- or C_2), leaving each with an unmodified lysine as an alternate conformation. Further model building and refinement was completed using Coot and Refmac. Hydrogens were added during refinement, and anisotropic *B*-values were calculated. Final models were validated using the JCSG quality control server incorporating Molprobity, ADIT (http://rcsb-deposit.rutgers.edu/validate) WHATIF, Resolve, and Procheck. Data collection and refinement statistics are displayed in Table S2.

3. RESULTS AND DISCUSSION

Designing Covalent TTR Kinetic Stabilizers

To circumvent liberating a potentially toxic leaving group during the irreversible modification of TTR by our previous covalent kinetic stabilizers comprising thioesters and esters (e.g., **1**, Figure 3)[44,45], we chose to use the sulfonyl fluoride functional group as the electrophile. The sulfonyl fluoride generates a benign fluoride ion leaving group upon attack by the K15 ε-amino group of TTR.

Originally proposed by Baker et al. for the covalent modification of dihydrofolate reductase[64], the aromatic sulfonyl fluoride group possesses the remarkable ability to remain relatively inert to nucleophilic substitution until anchored in an activating binding site. Baker proposed that this unique reactivity is a consequence of the highly solvated nature of the sulfonyl fluoride functional group[65,68]. However, our observation that the sulfonyl

fluoride group behaves like a non-polar substituent on thin layer chromatography plates and the like calls this hypothesis into question. Instead, we hypothesize that the formation of the reversible TTR•kinetic stabilizer complex (Figure 2, top panels) permits the simultaneous stabilization of the fluoride ion leaving group and attack of the incoming nucleophile at the sulfur VI center. Therefore, it is the ability of a binding site to facilitate a medley of concurrent interactions that accounts for the change in reactivity of the sulfonyl fluoride group when anchored in a protein binding pocket. This reaction requires the assistance of hydrogen bonds between the hard, electron-rich, nascent fluoride ion and either a water molecule (not shown) or, more likely, a protein hydrogen bond donor (Glu54 shown) present in the TTR T_4 binding pocket. The resulting polarized and activated sulfonyl fluoride (Figure 2, top right panel) is thus susceptible to attack by a proximal nucleophile, especially Lys15 in TTR. The reactive nature of the activated sulfonyl fluoride requires that it be aligned within the binding pocket to react with the desired side chain nucleophile, or risk unwanted hydrolysis to the sulfonic acid (Figure 2, left panels). In our case, we hypothesized that the pK_a-perturbed ε-amino group of K15 would act as the nucleophile, while the proton from the salt bridge between K15′ and E54′ (see below and Figure 9), or a water molecule held in a H-bonding network within the T_4 pocket may activate the sulfonyl fluoride, leading to the formation of a sulfonamide linkage of the 1,3,4-oxadiazoles to TTR[27,69,70].

Having decided to use the sulfonyl fluoride functional group as an activatable electrophile, we focused on designing a substructure capable of positioning the reactive functionality in an optimal position relative to the pK_a-perturbed K15 ε-amino group within the TTR T_4 binding pocket. TTR kinetic stabilizers are typically comprised of two differentially substituted aromatic rings (aryl ring A and aryl ring B), connected via a linker (Figure 1c)[27,46,48-50]. Through examination of the previously reported crystal structure of the benzoyl substructure of **1** (Figure 3) covalently bound in the T_4 binding pocket of TTR[44], we hypothesized that if aryl ring B of **3-18** were to bind at the base of the T_4 binding pocket, through interactions with S117/117′ and/or HBP3 and/or 3′ (Figure 1b), then a 1,3,4-oxadiazole linker would properly position a sulfonyl fluoride group substituted at the *meta* position of aryl ring A. In this orientation, the sufonyl fluoride functional group is proximal to the ε-amino group of K15, allowing for the rapid formation of the sulfonamide linkage upon activation of the sulfonyl fluoride[27,69-71]. Further analysis suggested that substituents at the *ortho* position of aryl ring A might interact with the residues comprising HBP1, further constraining the positioning of the sulfonyl fluoride with respect to the K15 nucleophilic side chain. The 1,3,4-oxadiazole scaffold is a frequently occurring structural motif in drug-like molecules, with a number of late stage clinical development candidates and one FDA-approved therapeutic containing this substructure[61,72].

Grounded on the structure-based design principles outlined above[37-55,69,70], 1,3,4-oxadiazoles **3-18** were synthesized (Figure 3). It should be noted that the inert nature of the unactivated sulfonyl fluoride to nucleophilic attack permitted the incorporation of this latent electrophilic group early in the synthesis[66]. This is in contrast to the situation for other reactive functional groups often used for the covalent modification of proteins that must be inserted at, or near, the end of a synthetic sequence[44,45]. This ability to carry the sulfonyl fluoride group through a range of reaction conditions allows greater flexibility when designing a synthetic sequence, thereby improving synthetic flexibility. The purity of the compounds utilized for the studies within was ≥ 95% (Table S4).

The aromatic sulfonyl fluoride library was designed to probe a range of structural features. Substituents in the 3 and 5 positions of aryl ring B are homologous to the iodines of the endogenous ligand T_4, and were anticipated to interact with the HBP 3/3′ at the base of the T_4 binding pocket (Figure 1b). Therefore, compounds **3-8** were included in the library to probe the effect of a) removing these substituents, **3**; b) varying the halogen atoms, **4- 7**; and

c) inserting methyl groups, **8**—substitutions that have proven to be instructive in previous structure-activity relationship studies. The phenol group situated in the *para* position of aryl ring B is a feature of several, but not all, TTR kinetic stabilizers. To investigate the effect of removing or modifying the phenolic functionality, we synthesized compounds **9-13**. The hydroxy group is removed in **9** and **10**, as is the possibility of forming a hydrogen-bonding network with S117/117′ present at the base of the T_4 binding pocket (Figure 1b), while **11** probed the effect of replacing the oxygen with a nitrogen atom[69-71]. Oxadiazoles **12** and **13** incorporated groups capable of acting as hydrogen bond acceptors, but not donors.

To address binding interactions between substituents on aryl ring A and HBP1 and 1′, compounds **14-17** were synthesized. Finally, the sulfonyl fluoride group was transposed to the *para* position of aryl ring A in **18**, to determine what effect this change would have on the compound's ability to covalently modify TTR.

Evaluation of Covalent Modification of WT-TTR by the Candidate Kinetic Stabilizers

The efficiency with which the library depicted in Figure 3 covalently modifies WT-TTR was determined by HPLC analysis (Figures 4 and S1)[44]. Briefly, the oxadiaxoles (7.2 μM, the minimum concentration required to bind and react with both T_4 binding sites) were incubated with WT-TTR (3.6 νM tetramer) at pH 7.0 in buffer. After 18 h, the reaction mixtures were directly analyzed by HPLC, monitoring absorbance at 280 nM (Figure 4, taking into account the increased ε of the conjugate). Due to the tetrameric nature of TTR, when both T_4 binding pockets are occupied only two of the four monomer subunits can be covalently modified, thus, a maximum TTR monomer modification yield of 50% is possible. The compounds (14.4 μM) were also incubated with TTR (3.6 μM tetramer) at a 4:1 stoichiometry to investigate whether any non-specific covalent modification occurred. In all cases, neither HPLC nor LCMS detected any TTR conjugates other than those resulting from reaction between the sulfonyl fluoride of the covalent kinetic stabilizer and the ε-amino group of K15. For all compounds tested, when the percentage modification is below the theoretical maximum of 50%, the ligand mass balance can be accounted for by the recovered sulfonic acid resulting from sulfonyl fluoride hydrolysis. The formation of this hydrolysis product is attributed to poor alignment of the compound's sulfonyl fluoride group with the ε-amino group of K15, upon activation in the T_4 binding site. This allows the activated sulfonyl fluoride to react with water (Figure 2, left panels).

Compounds **3-8** reveal how substituents at the 3 and 5 position of aryl ring B influence the orientation and reactivity of the sulfonyl fluoride. When the substituents are H, **3**, or are too small to effectively orient the molecule at the base of the pocket, **4**, the amount of covalent modification is reduced (Figure 3). The larger chloride atoms at the 3 and 5 positions, **5**, improved the yield of modified WT-TTR to 48%, whereas increasing the size of the halogens further to bromo- or iodo-, **6** and **7**, reduced the amount of covalent modification. It is hypothesized that the presence of the larger halides prevent the oxadiazoles from adopting orientations within the binding pocket that allow for optimal alignment of the incoming nucleophile with the activated sulfonyl fluoride, thereby reducing the yield of conjugate formation. Utilizing 3,5 methyl groups, **8**, generates the orientation and the flexibility needed to facilitate the quantitative modification of TTR, consistent with the similar size of chloro and methyl. Importantly, when the phenol group is removed from the scaffold, affording compounds **9** and **10**, 48% and 50% covalent modification was observed, respectively. This excellent yield of covalent attachment to TTR is attributed to the removal of the interactions between the hydroxy group and serines at the base of the pocket[69,70]. This in turn presumably affords a greater degree of freedom within the binding pocket, which subsequently improves the efficiency of the conjugation reaction utilizing **9** and **10**. Replacing the hydroxy group with a bromine, **13**, (only capable of accepting a H-bond from

S117/117′) maintains the level of covalent linkage observed for di-bromide **10**. The same appears to be true for methyl ether **12**. In contrast, when an amine is substituted for the hydroxy group, **11**, the percentage of modification is reduced, implying that the nitrogen analogue is capable of forming hydrogen bonding interactions that interfere with the alignment of the sulfonyl fluoride with the K15 amino group.

The amount of covalent modification is also influenced by the insertion of substituents at the *ortho* position of aryl ring A, **14- 17**. The size and polarizability of the substituent appears to be important when determining the percentage of covalent modification observed, with chloride, **14**, and bromide, **15**, substituents yielding optimal results. In contrast to the chloro substituent, insertion of an isoteric methyl group at the 4-position of ring A, **17**, is not well tolerated, which may be due to the difference in polarizability.

Positioning the sulfonyl fluoride functional group in the *para* position of aryl ring A, **18**, is highly detrimental to the formation of the covalent conjugate[69,70]. We hypothesize this is due to the change in the alignment of the activated electrophile with the incoming nucleophile, thereby reducing the amount of conjugate formation and increasing the amount of sulfonyl fluoride hydrolysis.

We were next interested in investigating what effect removing K15 from the TTR binding pocket would have on the covalent modification of TTR. Thus, the aforementioned sulfonyl fluorides **3-18** (7.2 μM) were incubated, at pH 7, with K15A-TTR (3.6 μM tetramer), an unnatural TTR variant that lacks the nucleophilic pK_a-perturbed ε-amino group at the top of the T_4 binding pocket[44]. Interestingly, oxadiazoles that lacked a phenol group merely hydrolyzed in the presence of the K15A TTR homotetramer, presumably due to activation in the T_4 binding pocket. In contrast, compounds **4-6** and **14-15** formed up to 20 % covalent modification with the K15A mutant (Table S5), while the majority of the starting material hydrolyzed. To determine the site of covalent modification, a sample of K15A-TTR modified by **6** was digested with trypsin and the resulting peptides analyzed by LCMS-MS. This analysis demonstrated that **6** had modified either cysteine 10, generating a thiosulfonate, or lysine 11, generating a sulfonamide, nucleophilic residues situated at the top of the T_4 binding pocket. This result suggests that in the absence of the more favored K15 nucleophile the compounds that possess a phenol group are capable of forming alternative and dynamic binding interactions further up the TTR T_4 binding pocket, permitting such reaction with these residues. However, while the majority of the starting material hydrolyzed (Figure S2), a distinct reaction afforded the corresponding sulfinic acid (detected by LCMS). This product was attributed to the reduction of the thiosulfonate by the cysteine-10′ residue[73], thereby generating the observed sulfinic acid and di-sulfide linked K15A-TTR-monomers.

Investigation of the Kinetics of Covalent Modification of WT-TTR by 5, 9, and 15

Having demonstrated that the compounds can chemoselectively covalently modify WT-TTR, to a greater or lesser extent depending on the specific structural features of the oxadiazole being tested, we were next interested in determining the rate of the reaction. To this end, compounds **5**, **9**, and **15** were selected to investigate what difference removing the *para* phenol group from aryl ring B (**5** vs. **9**), and placing a substituent in the *ortho* position of aryl ring A (**5** vs. **15**) had on the rate of the reaction. The reactions were conducted as outlined above (WT-TTR tetramer: 3.6 μM, compounds: 7.2 μM), at 37 °C, and an aliquot of the reaction mixture was quenched with TFA at 2, 10, 30, 60 min, and 120 min. The amount of covalent modification as a function of time was determined by reverse phase HPLC analysis (Figure 5).

From these data it can be seen that **5**, **9**, and **15** generated the covalent linkage much faster than the previously published covalent kinetic stabilizer **19** (t_{50} ~20 min)[45]. We believe that this difference in rate is attributable to two factors. First, the bulky thioester retards the binding of **19** in the T_4 binding pocket, and subsequently decreases the rate of covalent modification. Secondly, upon activation in the binding site, the sulfonyl fluoride moiety is far more reactive than the thioester and thus undergoes displacement at an accelerated rate. Moreover, an interesting relationship between structure and the rate of reaction was observed for **5**, **9**, and **15**. While both **5** and **15** generated the sulfonamide linkage at approximately the same rate (t_{50} ~ 1 min), **9** was slightly slower to react (t_{50} ~4 min). The *para* phenol group, present in **5** and **15** appears to accelerate the rate of covalent TTR modification by influencing the binding pre-equilibrium and/or the reaction geometry.

To further quantify the kinetics of covalent modification of TTR by **5**, we examined the time-dependent increase in fluorescence upon mixing **5** and WT TTR. This experiment was performed under pseudo-first order conditions, with **5** present at a concentration of 10 nM and TTR in large excess (200, 400, 600, and 800 nM). In all cases, the increase in fluorescence was single exponential; however, the observed rate constant (k_{obs}) had a hyperbolic dependence on the TTR concentration (Figure S3), consistent with a rapid prior binding equilibrium before the covalent modification step[74]. Fitting the k_{obs} vs. [TTR] data to such a model (see Supporting Information) yielded a K_d = 400 ± 90 nM, $k_{covalent}$ = 0.024 ± 0.002 s^{-1}.

Finally, we were interested in monitoring the rate of hydrolysis of the sulfonyl fluoride in the absence of WT-TTR. Therefore, **5** (7.2 μM) was dissolved in buffer (pH 7) at 37 °C, and an aliquot taken every hour for the first 12 h and at 24 and 48 h and analyzed by RP-HPLC (Figure S4). From these data it can be seen that **5** slowly hydrolyzes to the corresponding sulfonic acid over a 48 h period, a rate too slow to interfere with the covalent modification of WT-TTR.

Inhibition of Acid-Mediated WT-TTR Amyloid Formation by Covalent Kinetic Stabilizers

We next investigated the ability of the sulfonyl fluorides **3-18** to inhibit WT-TTR amyloidogenesis under previously established acidic-mediated fibril forming conditions (accelerates amyloidogenesis to a convenient laboratory timescale)[22,28]. The oxadiazoles were incubated with WT-TTR tetramer (3.6 μM) for 1 h at a 2:1 or 1:1 ratio. Subsequently, the pH was adjusted to 4.4 and the resultant solution incubated at 37 °C. After 72 h, it has been demonstrated that 90% of WT-TTR is aggregated in the absence of a kinetic stabilizer. The extent of aggregation was quantified by measuring the turbidity of the samples, an approach that has been demonstrated to be equivalent to thioflavin T-based quantification, and is recorded as a percentage relative to WT-TTR (100%) (Figure 3)[32]. Potent kinetic stabilizers of WT-TTR exhibit <10% aggregation under these conditions[11,39,43,44].

Oxadiazoles **3-18** all exhibited <10% aggregation when preincubated at 2:1 TTR tetramer stoichiometry (Figure 3). Five oxadiazoles (**4**, **5**, **11**, **14**, and **15**), when preincubated with the WT-TTR tetramer at 1:1 stoichiometry, yielded ≤ 10% TTR fibril formation after 72 h. Further studies on these in comparison to the poorer performers will be required to understand the mechanistic basis for these effects. Considerations include the extent of negative cooperativity in non-covalent binding, which determines the fraction of tetramers that have two covalent ligands bound vs. none; the relative rates of TTR tetramer modification vs. sulfonyl fluoride hydrolysis (the hydrolysis products also bind to the T_4 binding site blocking covalent modification while acting as kinetic stabilizers); the potency of ground state stabilization; and potentially other factors. Even in the absence of these further mechanistic insights, it is clear that modification of only one binding site using **4**, **5**,

11, **14**, and **15** is sufficient to kinetically stabilize the entire tetramer against amyloidogenesis. This observation is consistent with published results showing that covalently modifying one of the two T_4 binding pockets with a kinetic stabilizer is sufficient to kinetically stabilize the entire tetramer[30]. We anticipate that **4**, **5**, **11**, **14**, and **15** exhibit a high degree of negative cooperativity in terms of non-covalent binding and rapid conjugate formation, verified experimentally for **5** and **15**. We hypothesize that in the case of **4**, **11**, and **14**, the ability to highly stabilize (<10% aggregation) the tetramer against amyloidogenesis at a 1:1 ratio of compound to TTR, is due to significant negative cooperativity in non-covalent binding causing the covalent modification of one T_4 binding pocket per tetramer. This finding suggests that the dosage of the TTR stabilizer can be minimized, while still highly stabilizing the tetrameric form of WT-TTR.

Investigation into the Mechanism of WT-TTR Stabilization by Covalent Modification

The rate of formation of TTR fibrils is limited by the rate of dissociation of the tetramer[14,22,24,75]. This rate can be measured using far-UV circular dichroism (CD) or fluorescence spectroscopy, by linking the slow tetramer dissociation step to rapid and irreversible monomer unfolding at a high chaotrope concentration[14,23,30,37]. This provides valuable information about the degree of kinetic stabilization bestowed on the tetramer by a specific kinetic stabilizer[43].

To further investigate the kinetic stabilization exhibited by compounds **5**, **9**, and **15** (36 μM), these were preincubated with WT-TTR (18 μM tetramer) for 1 h, a period sufficient for all to react quantitatively with TTR (Figure 5)–thus conjugation kinetics are eliminated as a factor. The resultant solutions were subsequently diluted with urea (final urea concentration 6 M, final WT-TTR concentration 1.8 μM) to accelerate the rate of dissociation, and allow measurement on a convenient timescale[23,30]. The rate of tetramer dissociation was monitored by thermodynamically linking it to irreversible monomer unfolding of WT-TTR at 25 °C, using far-UV CD over 144 h (Figure 6).

As expected from the potent inhibition of acid-mediated amyloid fibril formation (Figure 3), all three kinetic stabilizers vastly increased the stability of tetrameric WT-TTR (Figure 6). Both **5** and **15** maintained greater than 90% of the tetrameric form of TTR even after incubation for 144 h in the presence of 6 M urea, while **9** retained 85% of the tetrameric structure. It is clear that these oxadiazoles prevent the formation of aggregates through kinetic stabilization of the WT-TTR tetramer[14].

Covalent Modification and Stabilization of the V30M-TTR

As mentioned above, V30M-TTR is the most common destabilizing mutation associated with FAP, a peripheral neuropathy that often exhibits autonomic nervous system involvement[5,9]. A previous study demonstrated that tafamidis, a non-covalent small molecule kinetic stabilizer of V30M-TTR, not only exhibited kinetic stabilization and fibril inhibition selectively *in vitro*[39], but also slowed the progression of V30M neuropathy progression in a phase II/III placebo-controlled clinical trial[12]. Thus, the ability of compounds **3**-**18** to covalently modify V30M-TTR homotetramers and slow aggregation was evaluated at 2:1 TTR tetramer stoichiometry (Figure 3). Due to the structural similarities between WT-TTR and the V30M variant, the compounds performed in an almost identical fashion, kinetically stabilizing V30M-TTR homotetramers. Thus, it is reasonable to anticipate that these compounds would also kinetically stabilize additional destabilized variants of TTR that are associated with polyneuropathies and cardiomyopathies.

Evaluating Modification of WT-TTR by Covalent Kinetic Stabilizers in Human Blood Plasma

From the 16 compounds synthesized in this study, sulfonyl fluorides **5**, **8**, **9**, **14**, **15**, and **16** were pursued further to investigate their ability to covalently modify TTR in blood plasma over the 4000+ other proteins present[44,63]. It is noteworthy that these compounds had all yielded near quantitative modification *in vitro* (Figure 3).

Using an ELISA assay kit (AbCam, Cambridge MA) the WT-TTR concentration in human blood plasma was established to be ~6.4 μM. The candidate kinetic stabilizers **5**, **8**, **9**, **14**, **15**, and **16** were subsequently incubated with plasma at three different concentrations, 6.4, 12.8, and 25.6 μM representing 1:1, 2:1 and 4:1 stoichiometric ratios (37 °C). Quantification of WT-TTR covalent modification was accomplished using a modification of the previously established *ex vivo* TTR plasma binding selectivity assay as detailed in the experimental section[63]. Covalent kinetic stabilizers **5**, **8**, **14**, **15**, and **16** produced the desired TTR-compound conjugate, and in agreement with the *in vitro* data, compound **16** performed worse than the other compounds tested (Figure S5). While compounds **5**, **14**, and **15** produced greater amounts of covalent modification (Table 1), surprisingly in each case the 4:1 and 2:1 ratio produced the same amount of conjugate (within error), while the 1:1 ratio produced only slightly less of the TTR-compound conjugate (Figures 7, S6, S7 and S8).

Therefore, there exists an apparent upper limit of modification of TTR by **5**, **14**, and **15** of ~35% (Figures S6, S7 and S8). When the same compounds were dosed at a 1:1 stoichiometry ~25% of the TTR, i.e., one T_4 binding site per TTR tetramer, is modified (considering the error of the ELISA assay). Covalent modification of one of the T_4 binding sites in the TTR tetramer was shown to be very effective at preventing aggregation (>90%) in the acid-mediated fibrillization assay[30,75].

Sulfonyl fluoride **8** underperformed when compared to the amount of covalent modification observed *in vitro*, suggesting that the 3, 5 halide groups of aryl ring B are an important structural feature to gain chemoselective modification over the +4000 other proteins present in the blood (Figure S9). Interestingly, despite the formation of a near quantitative amount of covalent modification *in vitro*, **9** failed to generate enough TTR-compound conjugate in plasma to quantify, regardless of the stoichiometries employed (Table 1 and Figure S10). From these data, it is seems that the incorporation of a *para* hydroxy group on aryl ring B is required to ensure covalent modification of TTR in blood plasma. The reason for this is believed to be two-fold. First, the hydroxy group forms a key binding interaction in the T_4 binding pocket, thus increasing the affinity of the compound for TTR and slowing the off-rate, providing more time for conjugation. Secondly, the hydroxy group increases the compound's hydrophilicity, helping to prevent the sequestering of the compound by hydrophobic regions present in the ≈ 4000 other proteins found in blood plasma.

Addition of **5** (8.9 μM, 1.44 mM) to human blood plasma (1 mL) afforded intrinsic fluorescence when visualized with a hand-held UV lamp after 1 h (Figure S11a) and a significant increase in fluorescence when evaluated in a fluorescence spectrophotometer (Figure S11b).

Crystallographic Analysis of WT-TTR• (Kinetic Stabilizer)$_2$ Conjugates

Crystal structures of the conjugation products resulting from the reaction between recombinant WT-TTR and sulfonyl fluorides **5**, **9**, and **15** were determined at 1.40, 1.46 and 1.22 Å resolution, respectively (see Table S2 for data collection and refinement statistics). In all three structures, the electron density was clear and allowed unambiguous placement of the organic substructure in the unbiased 2*F*o - *F*c electron density maps and identified the sulfonamide linkage between the sulfonyl fluoride and the ε-amino group of K15. The 3,5-

dichlorophenyl ring of **9** binds within the inner binding cavity where the chlorine atoms are placed into HBP3 and 3′, bridging adjacent TTR subunits (Figure 8a). The addition of a 4-hydroxy group to this ring (as seen in **5** and **15**) allows further hydrogen bonding with S117/117′ at the base of the T_4 binding site (Figure 8b and c). Although both **9** and **5** are efficient at covalently modifying TTR *in vitro*, we hypothesize that it is the extra interactions that affords **5** greater selectivity *ex vivo*. While the 1,3,4-oxadiazole ring linking the aryls does not appear to interact with any residues within the T_4 binding site, it does afford rotational flexibility to aryl ring A, optimally positioning the sulfonyl fluoride group for activation and subsequent attack from the pK_a-perturbed K15 nucleophile. The addition of a bromine atom *para* to the sulfonyl fluoride group as seen in **15,** fits neatly into HBP1 or 1′. Biochemical data suggest either a chlorine or bromine in this position to be preferred (Figure 3). Addition of the bromine at this position has the effect of displacing the ring slightly further into the center of the pocket (Figure 8 and Figure S12).

Structure-based Hypotheses for Sulfonyl Fluoride Activation

To gain insight into the structural basis for sulfonyl fluoride activation within the T_4 binding site, sulfonyl fluoride **15** was computationally modeled in the T_4 pocket. The *in silico* docking of **15** was completed using the "Dock simulation" algorithm employing the 'induced fit' protocol in the program MOE (Molecular Operating Environment 2011.10, Chemical Computing Group, Montréal, Canada). Briefly, the high-resolution coordinates for the sulfonamide resulting from the reaction of **15** with WT-TTR (PDB: 4FI8) were used as the TTR receptor coordinates.

For the simulation, all water molecules were removed and the target pocket was defined as residues within 8 Å of the bound ligand **15**. The ligand conjugated lysine was then removed prior to the docking simulation leaving only the alternate, unconjugated lysine conformation. Hydrogens were included in the simulation and their positions optimized using the Protonate 3D function within MOE, which calculates and assigns protonation from a discrete collection of states. The Generalized Born/Volume Integral (GBVI) electrostatics model was used for longer-range interactions and solvation effects[80,81]. By default the TTR backbone atoms are held fixed during refinement, but side chains of TTR within the defined pocket are partially tethered, which allows freedom around rotational bonds. In the 'induced fit' protocol, the weights of the tethers are determined from the individual atom temperature factors (*B*-values) allowing the residue side chains rotational freedom to move. The molecular mechanics force field MMF94x was employed to optimize TTR–**15** interactions and the best poses were scored using the London dG and GBVI/VSA dG (Generalized Born Volume Integral/Van der Waals Surface Area) scoring functions. For full details of the docking methodology and scoring functions see Supporting Information.

The top scoring pose correctly places **15** in an almost identical position as in the sulfonamide conjugate in the experimentally determined X-ray structure (Figure 9). In this optimized pose, K15 and E54 form a salt bridge, while K15′ is seen to interact with the sulfonyl fluoride functional group. This H-bonding to the sulfonyl fluoride group appears to activate it, enabling the pKa-perturbed K15 to attack via an S_N2 like mechanism starting at a distance of 3.6Å[82-85]. While it is unlikely E54′ will be protonated under physiological conditions, it is possible that the proton of the salt bridge, between K15′ and E54′, could provide the requisite hydrogen bond for activation of the sulfonyl fluoride. While solvent was excluded in this simulation, another possibility is that E54′ plays an important role in coordination of water molecules. It is entirely plausible that an ordered water molecule, as part of an internal network within the T_4 pocket, could be hydrogen bonding to the fluoride and therefore activating this group towards simultaneous K15 attack. Such ordered water molecules have been observed before in the high-resolution apo structures of TTR[86,87] and

also in the presence of a variety of liganded structures[39,50,88,89]. A final comparison of the modeled unconjugated ligand and final experimentally determined conjugated X-ray structure shows that very little conformational movement of either the ligand or TTR pocket takes place upon formation of the sulfonamide bond suggesting that the *meta* aryl sulfonyl fluoride functional group is optimally placed to undergo both activation and reaction within the T_4 pocket (Figure 9). This is further supported by the evidence of poor reactivity of **18**, containing the sulfonyl fluoride group in the *para* position of aryl ring A, which is then inaccessible to the K15 nucleophile.

Covalent Modification of WT-TTR Creates Green Fluorescent Conjugates

Compounds **3-8**, **11**, **14-16**, and **18** all produced varying degrees of green fluorescence upon covalent modification of the TTR tetramer (Table S1). It should be noted that all of these compounds possess auxochromic substituents at the *para* position of aryl ring B. These substituents are capable of forming a hydrogen-bonding network with the S117/117′ residues at the base of the T_4 binding pocket. In comparison to the previously reported TTR covalent modifier**19** ($\lambda_{max\ ex}$ = 328 nM, $\lambda_{max\ em}$ = 430 nM; Figure 5), the emission spectra of these compounds were all substantially red shifted (excitation: 313-365 nM, emission: 510-556 nM). The quantum yields of the conjugates afforded by TTR modification employing **5** and **6**, were determined to be 0.19 and 0.20 respectively, compared to 0.00 in buffer alone–the data for **5** illuminated by a UV lamp (Figure S13) is consistent, as is the data in Table S1[45]. The quantum yields of the remaining compounds were not determined because their fluorescence spectra were either comparatively weak or the compounds did not exhibit a high extent of covalent modification (Table S1 and Figure 3).

Investigating the Origins of Conjugate Fluorescence

In an effort to determine whether the generation of green fluorescence simply requires binding (very fast) or requires binding and covalent modification, **5** (7.2 μM) was incubated at 37 °C with WT-TTR (3.6 μM) and the fluorescent spectra recorded every 6 sec. The rate of emergence of the fluorescence was compared to the rate of covalent modification according to RP-HPLC analysis (Figure S14). From these data, a correlation exists between the rate of increase of fluorescence and the rate of covalent modification, suggesting that rapid non-covalent binding of the sulfonyl fluoride is insufficient to afford maximal red-shifted fluorescence. The fluorescence spectra of K15A-TTR treated with compounds **3-6**, **14** and **15** were also recorded. The fluorescence intensities were substantially diminished (Table S1), consistent with the inability to covalently modify K15 (Table S5). Moreover, the signals were blue shifted (emission: 490-510 nM) compared to the WT-TTR conjugation (emission: 520 nM), suggesting that covalent conjugation directly influences the red-shifted fluorescence emission spectrum of the covalently bound fluorophore (Figure 10a).

To probe the origins of conjugate fluorescence further, two analogs of **5** were prepared: the sulfonic acid **5a** (resulting from hydrolysis of **5**) and N-methyl sulfonamide **5b** to mimic the sulfonamide linkage of **5** to WT-TTR. While the fluorescence intensity of **5b** ($\lambda_{max\ ex}$ = 355 nm, $\lambda_{max\ em}$ = 515 nm) bound to WT-TTR (Figure 10c) is comparable to fluorescence intensity of the WT-TTR conjugate resulting from treatment with **5**, the fluorescence intensity of **5a** ($\lambda_{max\ ex}$ = 342 nm, $\lambda_{max\ em}$ = 507 nm) bound to WT-TTR is almost twice as intense (Figure 10b). The quantum yields of WT-TTR complexes with **5a** and **5b** were determined to be 0.13, similar to the value found for the WT-TTR conjugate resulting from treatment with **5**. The quantum yields of **5a** and **5b** in buffer alone were determined to be 0.00. Interestingly, the maximum emission wavelength of the complexes of **5**a and **5**b with WT-TTR did not achieve the red shift exhibited by the conjugate formed by the reaction between WT-TTR and **5**. While it is clear that **5**a and **5**b binding to WT- and K15A-TTR can yield fluorescence, we hypothesize that binding of **5** to WT-TTR and sulfonamide

formation is required to recapitulate the intensity and red-shifted fluorescence of the covalent conjugate. Although there is certainly future mechanistic work remaining, to our knowledge, the described molecules are the first example of protein-selective, environmentally sensitive, push-pull fluorophores.

The structural similarity of **5** and its analogs to some known environmentally (solvent) sensitive push-pull fluorophores prompted us to probe the fluorescence intensity of **5**, **5a**, **5b** in solvents of variable polarity[90]. Compounds **5** and **5b** were found to have high fluorescent intensity in non-polar solvents (toluene, dioxane and chloroform). Fluorescence intensity was diminished in polar solvents, being the lowest in water (Figure S15). Compound **5a** exhibited higher variability. It remained fluorescent in dioxane, ethanol and acetone. The fluorescent intensity of **5a** was decreased in chloroform and remained very weak in water, suggesting that factors other than solvent polarity influence the ability of **5a** to display fluorescent properties. The Stokes shifts of **5, 5a** and **5b** in organic solvents (Table S6) were significantly diminished (below 100 nm) in comparison to Stokes shifts observed for **5a**, **5b** and WT-TTR conjugates with **5** (on average, 160 nm). The only exception was observed when spectra of **5**, **5a** and **5b** were recorded in ethanol (Stokes shifts values from 150-190 nm). The solvent dependent data provide evidence that non-covalent binding to the hydrophobic pocket of WT-TTR may afford some fluorescence from the complex; however, the red-shifted, intense fluorescence resulting from the treatment of WT-TTR with **5** seems to require covalent conjugate formation.

Conclusions

In summary, we have generated a library of 1,3,4-oxadiazoles linking two aromatic rings, one of which incorporates a sulfonyl fluoride functional group. The best covalent kinetic stabilizers identified in this study were shown to bind the T_4 binding site of WT-TTR and react chemoselectively with the ε-amino group of K15, thereby generating a sulfonamide linkage. Covalent modification of the T_4 binding site was also demonstrated to highly stabilize the tetramer and prevent aggregation. In addition, three of the compounds efficiently modify WT-TTR in human blood plasma when dosed at a 1:1 stoichiometry, a ratio that effectively ameliorated aggregation *in vitro*. Several of the compounds also displayed fluorescence upon the formation of the covalent conjugate. Finally, three of the compounds were co-crystallized with WT-TTR and the high-resolution structures determined. These structures not only provided valuable information relating to the binding modes of the compounds, but also afford insights into the possible mechanisms by which the sulfonyl fluoride functionality undergoes activation in the binding site of TTR.

Supplementary Material

Refer to Web version on PubMed Central for supplementary material.

Acknowledgments

We acknowledge NIH grants DK046335 to J.W.K., U01NS058046 to K.B.S., and CA58896 and AI42266 to I.A.W.; the Skaggs Institute for Chemical Biology; and the Lita Annenberg Hazen Foundation for financial support. We are grateful to Colleen Fearns for carefully reading and editing the manuscript. We thank the General Clinical Research Cen ter of the Scripps Research Institute for providing human blood. Portions of this research were carried out at the Stanford Synchrotron Radiation Lightsource, a Directorate of SLAC National Accelerator Laboratory and an Office of Science User Facility operated for the U.S. Department of Energy Office of Science by Stanford University. The SSRL Structural Molecular Biology Program is supported by the DOE Office of Biological and Environmental Research, and by the National Institutes of Health, National Institute of General Medical Sciences (including P41GM103393) and the National Center for Research Resources (P41RR001209).

ABBREVIATIONS

CNSA	Central nervous system selective amyloidosis
CD	Circular dichroism
FAC	Familial amyloid cardiomyopathy
FAP	Familial amyloid polyneuropathy
HBP	Halogen binding pocket
SSA	Senile systemic amyloidosis
TTR	Transthyretin
WT	wild type

REFERENCES

1. Chiti F, Stefani M, Taddei N, Ramponi G, Dobson CM. Nature. 2003; 424:805. [PubMed: 12917692]
2. Dobson CM. Nature. 2003; 426:884. [PubMed: 14685248]
3. Hardy J, Selkoe DJ. Science. 2002; 297:353. [PubMed: 12130773]
4. Pepys, MB. Immunological Diseases. Samter, M., editor. Vol. 1. Little, Brown and Company; Boston \ Toronto: 1988. p. 631
5. Zeldenrust, SR.; Benson, MD. John Wiley & Sons, Inc.; 2010. p. 795
6. Chen CD, Huff ME, Matteson J, Page L, Phillips R, Kelly JW, Balch WE. EMBO J. 2001; 20:6277. [PubMed: 11707399]
7. Cohen FE, Kelly JW. Nature. 2003; 426:905. [PubMed: 14685252]
8. Solomon JP, Page LJ, Balch WE, Kelly JW. Crit Rev Biochem Mol Biol. 2012; 47:282. [PubMed: 22360545]
9. Andrade C. Brain. 1952; 75:408. [PubMed: 12978172]
10. Benson MD. TIBS. 1989; 12:88.
11. Coelho T, Chorao R, Sausa A, Alves I, Torres MF, Saraiva MJ. Neuromusc. Disord. 1996; 6:27. [PubMed: 8845715]
12. Coelho T, Maia L, Martins da Silva A, Waddington Cruz M, Planté-Bordeneuve V, Lozeron P, Suhr OB, Campistol JM, Conceição I, Schmidt HH-J, Trigo P, Kelly JW, Labaudinière R, Chan J, Packman J, Wilson A, Grogan DR. Neurology. 2012; 79:785. [PubMed: 22843282]
13. Hammarstrom P, Schneider F, Kelly JW. Science. 2001; 293:2459. [PubMed: 11577236]
14. Hammarstrom P, Wiseman RL, Powers ET, Kelly JW. Science. 2003; 299:713. [PubMed: 12560553]
15. Jacobson DR, Pastore RD, Yaghoubian R, Kane I, Gallo G, Buck FS, Buxbaum JN. N Engl J Med. 1997; 336:466. [PubMed: 9017939]
16. Westermark P, Sletten K, Johansson B, Cornwell GG 3rd. Proc Natl Acad Sci U S A. 1990; 87:2843. [PubMed: 2320592]
17. Blake CC, Geisow MJ, Oatley SJ, Rerat B, Rerat C. J Mol Biol. 1978; 121:339. [PubMed: 671542]
18. Foss TR, Wiseman RL, Kelly JW. Biochemistry. 2005; 44:15525. [PubMed: 16300401]
19. Monaco HL, Rizzi M, Coda A. Science. 1995; 268:1039. [PubMed: 7754382]
20. Wojtczak A, Cody V, Luft JR, Pangborn W. Acta crystallographica. Section D, Biological crystallography. 1996; 52:758.
21. Johnson SM, Connelly S, Fearns C, Powers ET, Kelly JW. J Mol Biol. 2012; 421:185. [PubMed: 22244854]
22. Colon W, Kelly JW. Biochemistry. 1992; 31:8654. [PubMed: 1390650]
23. Hammarstrom P, Jiang X, Hurshman AR, Powers ET, Kelly JW. Proc Natl Acad Sci U S A. 2002; 99(Suppl 4):16427. [PubMed: 12351683]

24. Hurshman Babbes AR, Powers ET, Kelly JW. Biochemistry. 2008; 47:6969. [PubMed: 18537267]
25. Jiang X, Buxbaum JN, Kelly JW. Proc Natl Acad Sci U S A. 2001; 98:14943. [PubMed: 11752443]
26. Jiang X, Smith CS, Petrassi HM, Hammarstrom P, White JT, Sacchettini JC, Kelly JW. Biochemistry. 2001; 40:11442. [PubMed: 11560492]
27. Johnson SM, Wiseman RL, Sekijima Y, Green NS, Adamski-Werner SL, Kelly JW. Acc Chem Res. 2005; 38:911. [PubMed: 16359163]
28. Lai Z, Colon W, Kelly JW. Biochemistry. 1996; 35:6470. [PubMed: 8639594]
29. Lai Z, McCulloch J, Lashuel HA, Kelly JW. Biochemistry. 1997; 36:10230. [PubMed: 9254621]
30. Wiseman RL, Johnson SM, Kelker MS, Foss T, Wilson IA, Kelly JW. J Am Chem Soc. 2005; 127:5540. [PubMed: 15826192]
31. Lee J, Culyba EK, Powers ET, Kelly JW. Nat. Chem. Biol. 2011; 7:602. [PubMed: 21804535]
32. Hurshman AR, White JT, Powers ET, Kelly JW. Biochemistry. 2004; 43:7365. [PubMed: 15182180]
33. Ng B, Connors LH, Davidoff R, Skinner M, Falk RH. Arch Intern Med. 2005; 165:1425. [PubMed: 15983293]
34. Westermark P, Bergstrom J, Solomon A, Murphy C, Sletten K. Amyloid. 2003; 10(Suppl 1):48. [PubMed: 14640042]
35. Falk RH. Circulation. 2005; 112:2047. [PubMed: 16186440]
36. Coelho T. Curr Opin Neurol. 1996; 9:355. [PubMed: 8894411]
37. Adamski-Werner SL, Palaninathan SK, Sacchettini JC, Kelly JW. J Med Chem. 2004; 47:355. [PubMed: 14711308]
38. Baures PW, Peterson SA, Kelly JW. Bioorg Med Chem. 1998; 6:1389. [PubMed: 9784876]
39. Bulawa CE, Connelly S, Devit M, Wang L, Weigel C, Fleming JA, Packman J, Powers ET, Wiseman RL, Foss TR, Wilson IA, Kelly JW, Labaudiniere R. Proc Natl Acad Sci U S A. 2012; 109:9629. [PubMed: 22645360]
40. Choi S, Kelly JW. Bioorg Med Chem. 2011; 19:1505. [PubMed: 21273081]
41. Green NS, Palaninathan SK, Sacchettini JC, Kelly JW. J Am Chem Soc. 2003; 125:13404. [PubMed: 14583036]
42. Petrassi HM, Klabunde T, Sacchettini J, Kelly JW. J. Am. Chem. Soc. 2000; 122:2178.
43. Razavi H, Palaninathan SK, Powers ET, Wiseman RL, Purkey HE, Mohamedmohaideen NN, Deechongkit S, Chiang KP, Dendle MT, Sacchettini JC, Kelly JW. Angewandte Chemie. 2003; 42:2758. [PubMed: 12820260]
44. Choi S, Connelly S, Reixach N, Wilson IA, Kelly JW. Nat. Chem. Biol. 2010; 6:133. [PubMed: 20081815]
45. Choi S, Ong DS, Kelly JW. J Am Chem Soc. 2010; 132:16043. [PubMed: 20964336]
46. Choi S, Reixach N, Connelly S, Johnson SM, Wilson IA, Kelly JW. J Am Chem Soc. 2010; 132:1359. [PubMed: 20043671]
47. Green NS, Foss TR, Kelly JW. Proc Natl Acad Sci U S A. 2005; 102:14545. [PubMed: 16195386]
48. Johnson SM, Connelly S, Wilson IA, Kelly JW. J Med Chem. 2008; 51:6348. [PubMed: 18811132]
49. Johnson SM, Connelly S, Wilson IA, Kelly JW. J Med Chem. 2008; 51:260. [PubMed: 18095641]
50. Johnson SM, Connelly S, Wilson IA, Kelly JW. J Med Chem. 2009; 52:1115. [PubMed: 19191553]
51. Johnson SM, Petrassi HM, Palaninathan SK, Mohamedmohaideen NN, Purkey HE, Nichols C, Chiang KP, Walkup T, Sacchettini JC, Sharpless KB, Kelly JW. J Med Chem. 2005; 48:1576. [PubMed: 15743199]
52. Peterson SA, Klabunde T, Lashuel HA, Purkey H, Sacchettini JC, Kelly JW. Proc Natl Acad Sci U S A. 1998; 95:12956. [PubMed: 9789022]
53. Petrassi HM, Johnson SM, Purkey HE, Chiang KP, Walkup T, Jiang X, Powers ET, Kelly JW. J Am Chem Soc. 2005; 127:6662. [PubMed: 15869287]

54. Purkey HE, Palaninathan SK, Kent KC, Smith C, Safe SH, Sacchettini JC, Kelly JW. Chem Biol. 2004; 11:1719. [PubMed: 15610856]
55. Razavi H, Powers ET, Purkey HE, Adamski-Werner SL, Chiang KP, Dendle MT, Kelly JW. Bioorg Med Chem Lett. 2005; 15:1075. [PubMed: 15686915]
56. Coelho T, Carvalho M, Saraiva MJ, Alves I, Almeida MR, Costa PP. J. Rheumatol. 1993; 20:179.
57. Kalgutkar AS, Dalvie DK. Expert Opin Drug Discov. 2012
58. Singh J, Petter RC, Baillie TA, Whitty A. Nat Rev Drug Discov. 2011; 10:307. [PubMed: 21455239]
59. Estebanez-Perpina E, Arnold LA, Jouravel N, Togashi M, Blethrow J, Mar E, Nguyen P, Phillips KJ, Baxter JD, Webb P, Guy RK, Fletterick RJ. Mol Endocrinol. 2007; 21:2919. [PubMed: 17823305]
60. Savi P, Pereillo JM, Uzabiaga MF, Combalbert J, Picard C, Maffrand JP, Pascal M, Herbert JM. Thromb Haemost. 2000; 84:891. [PubMed: 11127873]
61. Bala S, Kamboj S, Kumar A. J. Pharm. Res. 2010; 3:2993.
62. Alexander JP, Cravatt BF. Chem. Biol. 2005; 12:1179. [PubMed: 16298297]
63. Purkey HE, Dorrell MI, Kelly JW. Proc Natl Acad Sci U S A. 2001; 98:5566. [PubMed: 11344299]
64. Baker BR. Acc Chem Res. 1969; 2:129.
65. Baker BR. Annu. Rev. Pharmacol. 1970; 10:35. [PubMed: 4986559]
66. Dong, J.; Sharpless, B. Presented at the 243rd ACS National Meeting & Exposition 2012; San Diego, CA, USA. March 25;
67. Lashuel HA, Wurth C, Woo L, Kelly JW. Biochemistry. 1999; 38:13560. [PubMed: 10521263]
68. Baker BR, Hurlbut JA. J Med Chem. 1968; 11:233. [PubMed: 5654208]
69. Connelly S, Choi S, Johnson SM, Kelly JW, Wilson IA. Curr Opin Struct Biol. 2010; 20:54. [PubMed: 20133122]
70. Klabunde T, Petrassi HM, Oza VB, Raman P, Kelly JW, Sacchettini JC. Nat Struct Biol. 2000; 7:312. [PubMed: 10742177]
71. Hornberg A, Eneqvist T, Olofsson A, Lundgren E, Sauer-Eriksson AE. J Mol Biol. 2000; 302:649. [PubMed: 10986125]
72. Li Z, Zhan P, Liu X. Mini-Rev Med Chem. 2011; 11:1130. [PubMed: 22353222]
73. van Kasteren SI, Kramer HB, Jensen HH, Campbell SJ, Kirkpatrick J, Oldham NJ, Anthony DC, Davis BG. Nature. 2007; 446:1105. [PubMed: 17460675]
74. Espenson, JH. Chemical Kinetics and Reaction Mechanisms. 2nd ed.. McGraw-Hill; New York: 1995.
75. Wiseman RL, Green NS, Kelly JW. Biochemistry. 2005; 44:9265. [PubMed: 15966751]
76. Ando Y, Ohlsson PI, Suhr O, Nyhlin N, Yamashita T, Holmgren G, Danielsson A, Sandgren O, Uchino M, Ando M. Biochem Biophys Res Commun. 1996; 228:480. [PubMed: 8920938]
77. Ando Y, Suhr O, Yamashita T, Ohlsson PI, Holmgren G, Obayashi K, Terazaki H, Mambule C, Uchino M, Ando M. Neuroscience letters. 1997; 238:123. [PubMed: 9464635]
78. Bergquist J, Andersen O, Westman A. Clinical chemistry. 2000; 46:1293. [PubMed: 10973857]
79. Kishikawa M, Nakanishi T, Miyazaki A, Shimizu A, Nakazato M, Kangawa K, Matsuo H. Journal of mass spectrometry : JMS. 1996; 31:112. [PubMed: 8799265]
80. Labute P. J Comput Chem. 2008; 29:1693. [PubMed: 18307169]
81. Labute P. Proteins. 2009; 75:187. [PubMed: 18814299]
82. Sabol MM, Andersen KK. J Am Chem Soc. 1969; 91:3603.
83. Annunziata R, Colonna S, Cinquinni M. J Chem Soc Perkin Trans 1. 1972; 16:2057.
84. Johnson CR, Jonsson EU, Wambsgans A. J Org Chem. 1979; 44:2016.
85. Jones MR, Cram DJ. J Am Chem Soc. 1974; 96:2183.
86. Gales L, Saraiva MJ, Damas AM. Biochim Biophys Acta. 2007; 1774:59. [PubMed: 17175208]
87. Lima LM, Silva Vde A, Palmieri Lde C, Oliveira MC, Foguel D, Polikarpov I. Bioorg Med Chem. 2010; 18:100. [PubMed: 19954984]

88. Alhamadsheh MM, Connelly S, Cho A, Reixach N, Powers ET, Pan DW, Wilson IA, Kelly JW, Graef IA. Sci Transl Med. 2011; 3:97ra81.

89. Kolstoe SE, Mangione PP, Bellotti V, Taylor GW, Tennent GA, Deroo S, Morrison AJ, Cobb AJ, Coyne A, McCammon MG, Warner TD, Mitchell J, Gill R, Smith MD, Ley SV, Robinson CV, Wood SP, Pepys MB. Proc Natl Acad Sci U S A. 2010; 107:20483. [PubMed: 21059958]

90. Diwu Z, Lu YX, Zhang CL, Klaubert DH, Haugland RP. Photochem Photobiol. 1997; 66:424.

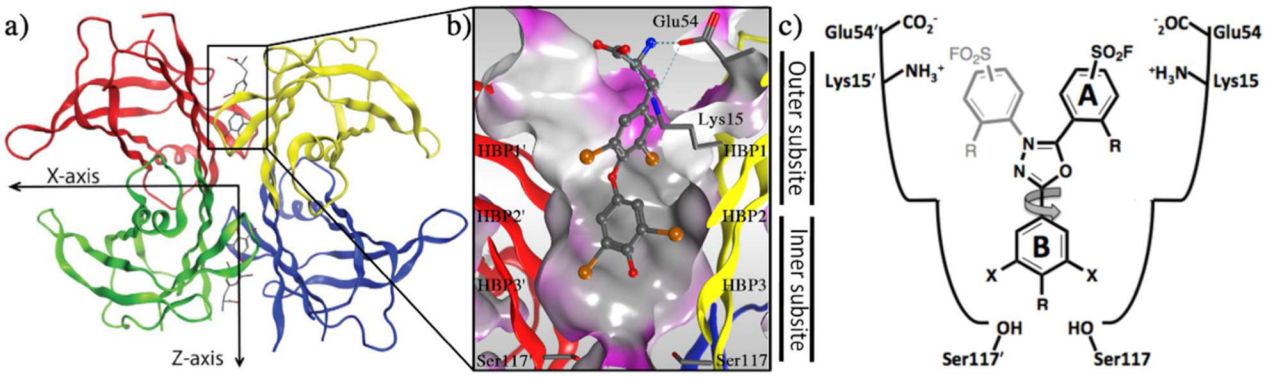

Figure 1.

Structure of homotetrameric WT-TTR with a focus on the T_4 binding pocket. **a)** Crystal structure of WT-TTR in complex with T_4 (2ROX) **b)** Close-up view of one of the two identical T_4 binding sites showing a ribbon depicted tetramer (colored by chain) with a "Connelly" molecular surface applied to residues within 8 Å of T_4 (hydrophobic = grey, polar = purple). The innermost halogen binding pockets (HBPs) 3 and 3′ are composed of the methyl and methylene groups of Ser117/117′, Thr119/119′, and Leu110/110′. HBPs 2 and 2′ are made up by the side chains of Leu110/110′, Ala109/109′, Lys15/15′, and Leu17/17′. The outermost HBPs 1 and 1′ are lined by the methyl and methylene groups of Lys15/15′, Ala108/108′, and Thr106/106′. These figures were generated using the program MOE (2011.10), Chemical Computing Group, Montreal, Canada. **c)** Schematic representation of the T_4 binding pocket with both the inner/outer binding subsites labeled and the amino acids that are being targeted in the design and optimization of substituents of aryl rings **A** and **B**. Rotation around the 1,3,4-oxadiazole ring linker gives rise to the symmetry related binding mode within the symmetrical T_4 pocket.

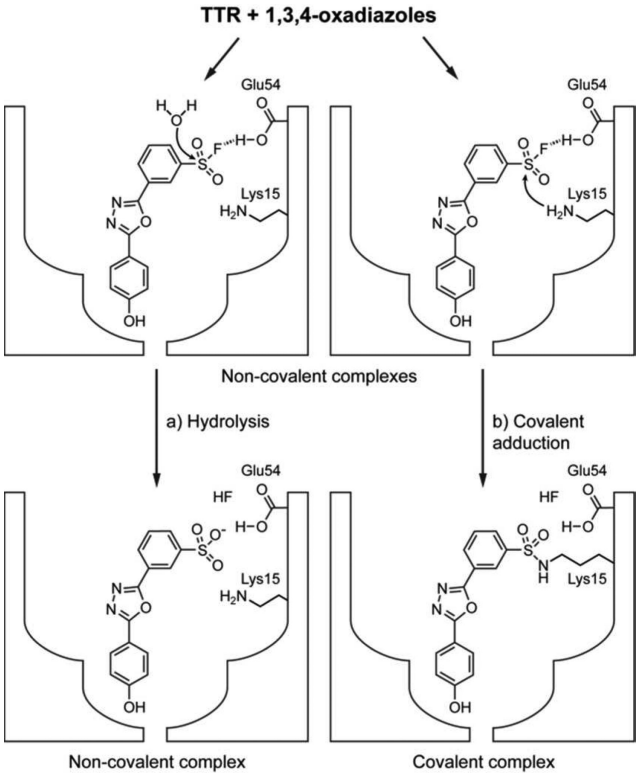

Figure 2.

An illustration of the potential fates of 1,3,4-oxadiazoles in the TTR binding pocket. TTR and 1,3,4-oxadiazoles initially form non-covalent complexes. Then the functional groups on the amino sides chains that line the binding pocket can catalyze either hydrolysis (path a) or covalent adduction (path b) by stabilization of the fluoride leaving group. In the Figure, we show Glu54 performing this function, but there are other possibilities, including the Glu 54 Lys15 salt bridge.

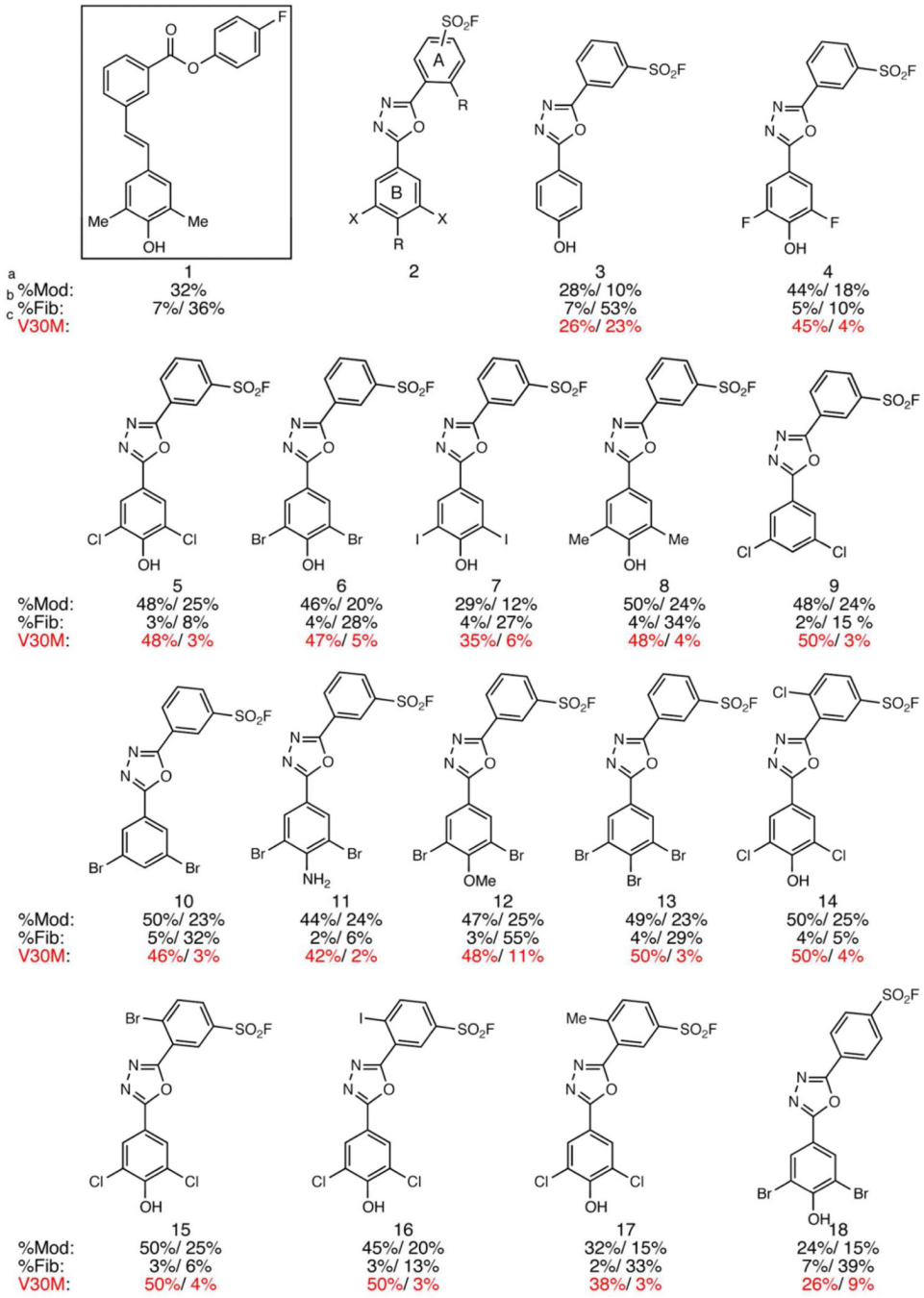

Figure 3.

Library of sulfonyl fluoride containing 1,3,4-oxadizoles. [a]Percentage modification of WT-TTR (black font) at 2:1/1:1 stoichiometries. 50% represents maximum covalent modification at 2:1 stoichiometry. [b] Percentage aggregation observed at 2:1/1:1 stoichiometries, compared to unstabilized WT-TTR (100%). [c] Percentage modification of V30M-TTR (red font) at 2:1 stoichiometry/ % aggregation observed at 2:1 stoichiometry. See Table S3 for error bars.

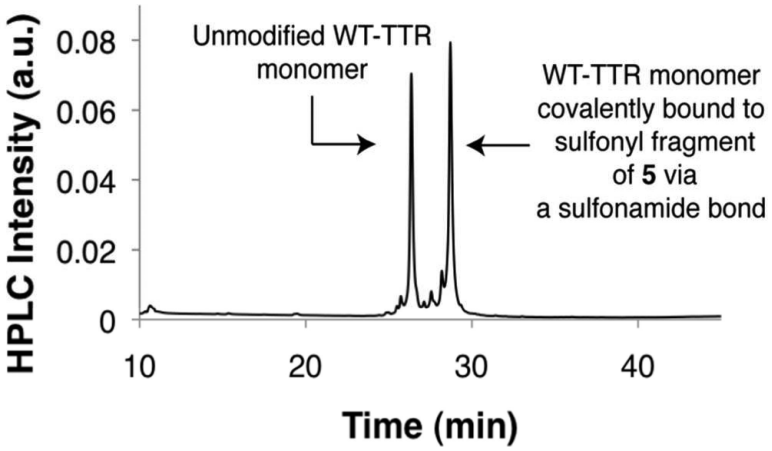

Figure 4.
Example C_{18}-RP HPLC analysis of WT-TTR pre-incubated with candidate covalent kinetic stabilizer **5**.

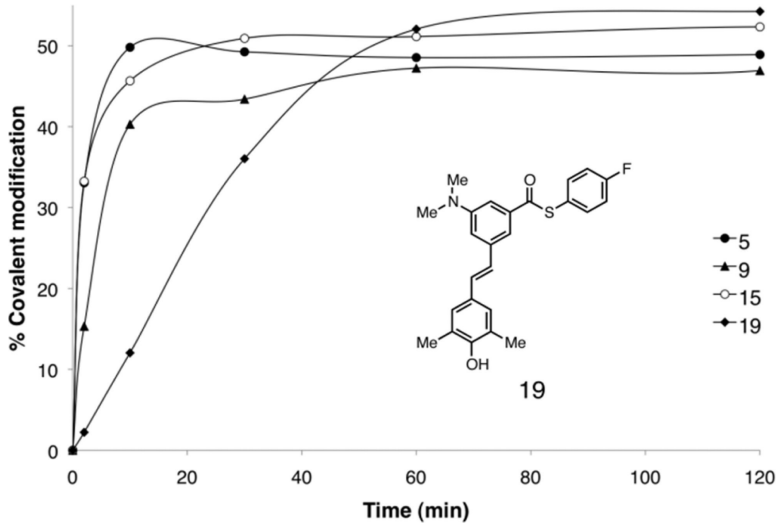

Figure 5.
Rate of WT TTR–(oxadiazole) conjugate formation analyzed by C_{18}-RP HPLC.

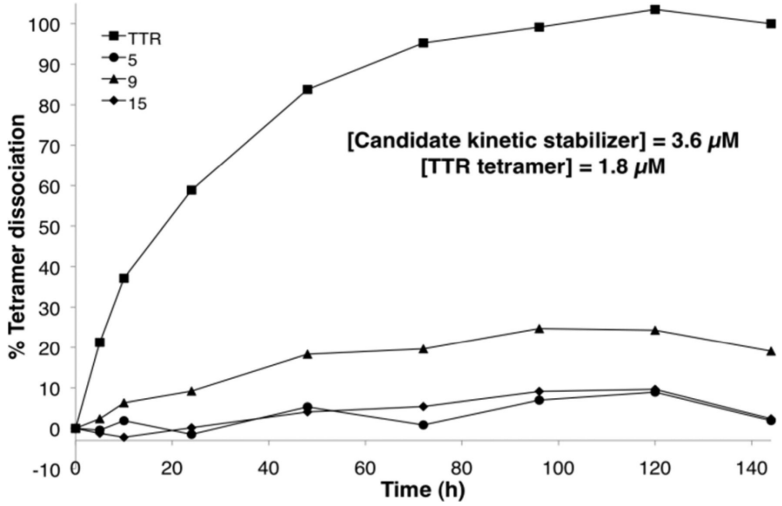

Figure 6.

Influence of covalent kinetic stabilizers **5**, **9**, (3.6 μM) on the rate of WT-TTR tetramer dissociation relative to WT-TTR (1.8 μM tetramer) in the absence of a covalent kinetic stabilizer. Dissociation and unfolding of TTR in 6 M urea is monitored by far-UV circular dichroism at 215 – 218 nM over 144 h after a 1 h preincubation period with covalent kinetic stabilizer.

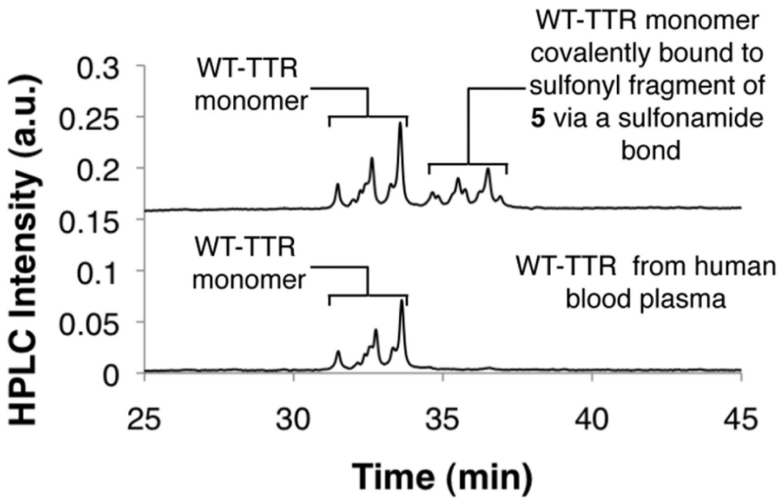

Figure 7.

Example C_{18}-RP-HPLC analysis of the modification of WT-TTR (6.4 μM) in human blood plasma by compound **5** (6.4 μM). Several oxidized Cys10 isoforms of TTR exist in human plasma, as ascertained by liquid chromatography and/or mass spectrometry[76-79]. Cys10 makes a mixed disulfide with the amino acid cysteine (TTR-Cys), the peptide glutathione (TTR-GSH), and the peptide cysteinylglycine (TTR-CysGly) and can be oxidized to S-sulfonated TTR.

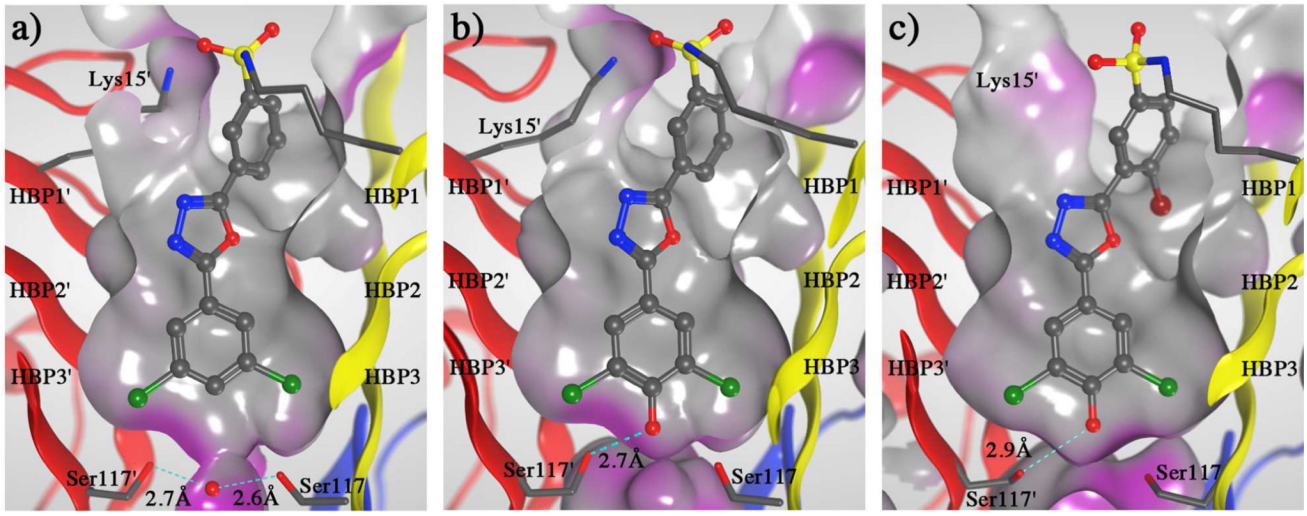

Figure 8.

Crystal structures of homotetrameric WT-TTR in complex with inhibitors **9, 5,** and **15** (panels a, b and c respectively). Close-up view of one of the two identical T_4 binding sites in a ribbon depicted tetramer colored by chain. A “Connelly” molecular surface was applied to residues within 8 Å of ligand in the T_4 binding pocket—hydrophobic (grey), polar (purple). The innermost halogen binding pockets (HBPs) 3 and 3′ are composed of the methyl and methylene groups of Ser117/117′, Thr119/119′, and Leu110/110′. HBPs 2 and 2′ are made up by the side chains of Leu110/110′, Ala109/109′, Lys15/15′, and Leu17/17′. The outermost HBPs 1 and 1′ are lined by the methyl and methylene groups of Lys15/15′, Ala108/108′, and Thr106/106′. Hydrogen bonds shown in light blue dashed lines, with the atomic distances labeled in Å. This Figure was generated using the program MOE (2011.10), Chemical Computing Group, Montreal, Canada.

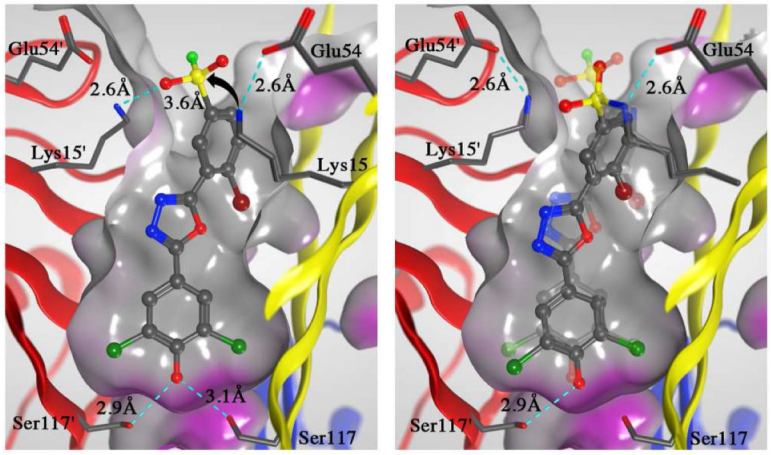

Figure 9.

Structural basis for sulfonyl fluoride activation. (Left) The docked structure of **15** into the T_4 binding site showing nucleophilic attack on the sulfonyl fluoride sulfur atom from the K15 ε-amino group as depicted by a black arrow. (Right) Crystal structure of homotetrameric WT-TTR as a conjugate after reaction with **15** and superposition of the unreacted docked conformation of **15** as a ghost view. Both show a close-up view of one of the two identical T_4 binding sites in a ribbon depicted tetramer colored by chain. A "Connelly" molecular surface was applied to residues within 8 Å of ligand in the T_4 binding pocket—hydrophobic (grey), polar (purple). Hydrogen bonds shown in light blue dashed lines, with the atomic distances labeled in Å. This Figure was generated using the program MOE (2011.10), Chemical Computing Group, Montreal, Canada.

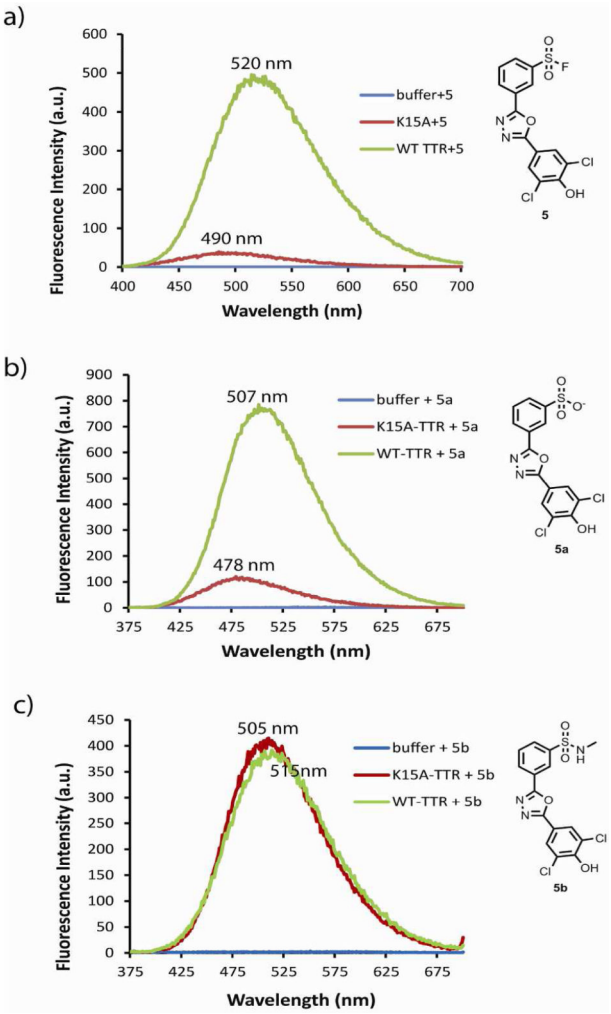

Figure 10.

Fluorescence emission spectra of compounds **5, 5a** and **5b** after 18 h incubation with WT- and K15A-TTR ($\lambda_{max\ ex}$ for **5**, **5a** and **5b** is 365, 342 and 355 nM, respectively).

Table 1

Percentage modification of WT-TTR (6.4 μM) in human blood plasma at the indicated 1:1, 2:1 and 4:1 stoichiometries of candidate kinetic stabilizers **5, 8, 9, 14, 15,** and **16**.

	% modification of WT-TTR in human plasma		
Compound	**1:1**	**2:1**	**4:1**
5	27	38	39
8	18	23	28
9	~0	~0	~0
14	26	34	34
15	23	33	33
16	14	20	19